Undergraduate Journal of Experimental Microbiology and Immunology (UJEMI) Vol. 28:1-13


# Investigating the inhibitory effects of ginsenoside Rg3 on the NLRP3 inflammasome in J774A.1 murine macrophage cells

Taylor Bootsma, Brandon Connor, Yugyoung Song, Claudia Szlavy

Department of Microbiology and Immunology, University of British Columbia, Vancouver, British Columbia, Canada

**SUMMARY** The nucleotide-binding domain, leucine-rich-repeat-containing family, pyrin domain-containing 3 (NLRP3) inflammasome is a multiprotein complex found in many myeloid cells that plays an important role in regulating the innate immune response. The NLRP3 inflammasome requires two signals to become fully activated; a pathogen-associated molecular pattern (PAMP) to prime the NF-KB pathway and a damage-associated molecular pattern (DAMP) to activate inflammasome formation. The priming of the NF-KB pathway results in the production of pro-IL-1β, pro-IL-18, and pro-caspase-1, along with a variety of other cytokines such as TNF-α. The activated NLRP3 inflammasome cleaves the pro-caspase-1 into mature caspase-1 which then cleaves the pro-Il-1β and pro-Il-18 into mature Il-1β and Il-18 respectively. The mature Il-1β and Il-18 can then leave the cell via secretion or pyroptosis. *Panax ginseng* is used widely in East Asian traditional medicine for its anti-inflammatory properties. Many of its medicinal properties are thought to come from ginsenoside Rg3 which is thought to play a role in regulating the NLRP3 inflammasome. In this study, we sought to develop a working model for the activation of the NLRP3 inflammasome in J774A.1 murine macrophage cells, and to investigate if Rg3 has inhibitory effects on the priming, activation, or both signals leading to NLRP3 inflammasome assembly. We were able to detect pro-IL-1β following treatment with LPS. Further, we were able to demonstrate the apparent down-regulation of TNF-α production in LPS-treated J774A.1 cells by ginsenoside Rg3.

## INTRODUCTION

The NLRP3 inflammasome is a multiprotein complex which plays a key role in inflammation (1). The NLRP3 inflammasome is highly expressed in myeloid cells, including dendritic cells and macrophages, and is an important contributor to the innate immune response (1, 2). NLRP3 inflammasome assembly is initiated by a broad range of extracellular, intracellular, and environmental signals. This is a 2-step process with priming occurring first, followed by activation. Priming can be initiated by stimulation of NOD-like receptors (NLRs)s, TOLL-like receptors (TLRs), or cytokine receptors on resting macrophages by PAMPs such as lipopolysaccharides (LPS), leading to the activation of the transcription factor NF-kB (3). NF-kB then upregulates inflammatory cytokines TNF-α, and other proteins involved in the inflammasome response such as NLRP3, pro-caspase 1, and pro-IL-1β (2). Once the cell has been primed, activation can be initiated by a variety of stimuli, including host, pathogen, and environment-derived antigens such as ATP or Nigericin, which is a microbial toxin derived from the gram-positive bacteria *Streptomyces hygroscopicus* (3, 4, 5). Upon stimulation, NLRP3 oligomerizes and recruits the adaptor protein ASC (apoptosis-associated speck-like protein containing a caspase recruitment domain). Assembled ASC recruits pro-caspase 1 causing proximity-induced caspase 1 self-cleavage and activation. Caspase 1 then cleaves pro-IL-1β and pro-IL-18 to mature IL-1β and mature IL-18 respectively. IL-1β and IL-18 are then released from the cell by either secretion or pyroptosis, and act as strong stimulators of inflammation in other cells (2). This release of IL-1β mediates the inflammatory response by recruiting neutrophils to the site of infection or injury, where they can either digest the pathogenic molecule, or recruit other immune cells to defend the host (6, 7). The cell cytoskeleton is also thought to play a role in the regulation of

**Published Online:** September 2023

**Citation:** Bootsma, Connor, Song, Szlavy. 2023. Investigating the inhibitory effects of ginsenoside Rg3 on the NLRP3 inflammasome in J774A.1 murine macrophage cells. UJEMI 28:1-13

**Editor:** Lauren Pugsley and Shruti Sandilya, University of British Columbia



Address correspondence to: https://jemi.microbiology.ubc.ca/

the NLRP3 inflammasome (8) as actin rearrangement has been associated with inflammasome formation (9).

As there are different types of inflammasomes found *in vivo* including the NLRC4 and AIM2 inflammasomes, the formation of the NLRP3 inflammasome does not seem to be specifically essential to host defense against pathogens (10, 11, 12). However, in diseases such as atherosclerosis, type 2 diabetes, gout and cryopyrin-associated periodic syndromes (CAPS), NLRP3 inflammasome activation, and its subsequent IL-1β production, play an important role in disease progression and severity (13, 14, 15, 16). Similarly, inflammation has been shown to interact with obesity in a pervasive cycle to exacerbate negative effects on health. It has been demonstrated that adipose tissue is a source of chemokines and proinflammatory cytokines, such as IL-1β, that exacerbate inflammation (17, 18). Further, studies have linked the NLRP3 inflammasome and obesity in a bidirectional fashion by showing that the inflammasome, and inflammasome-associated cytokines, impact the outcome of obesity. Specifically, it has been shown that NLRP3 and caspase 1 mediate adipocyte differentiation and adipogenic gene expression, which promote obesity (19, 20). The development of modern hygiene practices as well as the widespread use of antibiotics and vaccines has nearly doubled life expectancy since the 1700s (21). The decreased incidence of acute illness, and increased longevity, have been associated with an increased morbidity and mortality burden from chronic illnesses, including many age-related metabolic disorders (22, 23). According to Statistics Canada and the CDC, heart disease is the second leading cause of mortality in Canada and the first leading cause of mortality in the United States (24, 25). Type 2 diabetes and obesity are major risk factors for developing heart disease, and according to statistics Canada, in 2018 26.8% of Canadians were considered obese and another 36.3% were considered overweight (26). Together, this accounts for 17.2 million people in Canada alone. Additionally, according to Diabetes Canada, diabetes rates are continuing to rise with 5.7 million people in Canada currently diagnosed with diabetes (type 1 or type 2), and rates are showing no signs of leveling or decreasing (27). The rising frequency of metabolic-related diseases highlights the utmost importance of developing novel therapeutics and preventative treatments for these diseases. The NLRP3 inflammasome, responding to a diverse array of DAMPs associated with metabolic disease, is a promising target for the development of novel therapeutics (22).

Ginsenoside Rg3 is a chemical ingredient isolated from the traditional medicinal herb *Panax ginseng* which has been used widely in traditional Chinese medicine (28). Rg3 has been found to regulate blood vessel growth, decrease inflammation, and inhibit tumour growth (29, 30, 31, 32). Because of its pharmacological properties, Rg3 was approved by the Chinese Food and Drug Administration for treating non-small cell lung cancer in 2002 (31). Rg3 is believed to play an anti-inflammatory role through inhibition of the NLRP3 inflammasome, however, the mechanisms of this inhibition remain unclear. While some studies have shown that Rg3 has the ability to inhibit the priming step of the NLRP3 inflammasome, mediated through the NF-kB pathway (33, 34, 35), another study demonstrated that Rg3 may be able to directly inhibit NLRP3 oligomerization and subsequent NLRP3-ASC interactions (36). These studies indicate that Rg3 may be able to regulate the NLRP3 inflammasome through multiple mechanisms. Further characterization of the mechanisms by which Rg3 inhibits the NLRP3 inflammasome would allow for a better understanding of how Rg3 could be used as a novel therapeutic for metabolic-related diseases.

In this study, we aimed to test the effects of Rg3 on NLRP3 inflammasome activation. Firstly, we aimed to optimize the inflammasome activation model by treating J774A.1 murine macrophage cells with a range of nigericin concentrations at various time points following LPS stimulation. Secondly, to test the effect of Rg3 on NLRP3 inflammasome activation, we treated cells with Rg3 prior to and following LPS stimulation, and activated the inflammasome with the optimized nigericin stimulation conditions. As previous studies had difficulty detecting inflammatory cytokines released by inflammasomes (37, 38, 39), fluorescence microscopy of actin structures can provide an additional method of measuring inflammasome activation, therefore we used fluorescence microscopy to visualize the actin skeletons of each of our conditions by tagging the actin with an Alexa Fluor 568-Phalloidin conjugate, then used ImageJ to identify changes in the actin cytoskeleton (40). We predicted to see morphological changes in the actin skeleton following inflammasome activation, and

a lesser degree of change for the conditions pre-treated with Rg3 assuming it has an inhibitory effect on inflammasomes. We observed pro-IL-1β production in response to LPS priming of J774A.1 macrophages, yet we were unable to detect the cleaved mature protein in cell lysates. However, IL-1β was detectable in the supernatants, and thus this model shows promise to detect cleaved IL-1β production in future studies to measure inflammasome activation. Furthermore, we observed a lower production of TNF-α in response to Rg3 treatment, supporting that Rg3 is anti-inflammatory.

## METHODS AND MATERIALS

**Reagent Preparation.** LPS (*Escherichia coli*) (Sigma-Aldrich, Cat no. L4391) available in stocks of 1 mg/ml, was used for cell stimulation for signal 1. Nigericin from *Streptomyces hygroscopicus* (EMD Millipore, Cat no 481990) was resuspended in 95% ethanol at 5 mg/mL, and was used to stimulate the cell for signal 2. 1mg of ginsenoside Rg3 (Sigma-Aldrich Cat no. 64139) was dissolved in 200µl DMSO for final stock concentration of 5mg/mL.

**Cell Culture.** J774A.1 mouse macrophages (Kronstad Lab, Michael Smith Laboratories, UBC) were cultured in DMEMc media composed of Dulbecco's Modified Eagle Medium (DMEM), 10% Fetal Bovine Serum (FBS), and 2mM L-Glutamine (GlutaMax) (Thermo Fisher, Cat no. 35050061). The J774A.1 cells were at passage number 14 at the beginning of the experiment. Frozen cell stocks were created using DMEMc + 5% DMSO at 1.87 x $10^6$ to 3.39 x $10^6$ cells per cryovial. Cells were grown in an incubator at 37°C with 5% $CO_2$ in Thermo fisher EasYFlask tissue culture flasks (Thermo Fisher, Cat no. 156340) and Thermo fisher adherent cell plates (Thermo Fisher, Cat no. 140675) with the appropriate amount of media according to the manufacturer's instructions. The media was refreshed approximately every 2-3 days. The cells were passaged once they reached approximately 80-85% confluency. Frozen stocks of cells were thawed in a 37°C water bath and were given at least 48 hours to recover before changing media, passaging, or treatment.

**Stimulation of cells with LPS.** To verify successful priming by LPS, two wells of a 6-well plate with approximately 3.0 x $10^5$ J774A.1 cells per well were inoculated and grown for 24 hours. Cells were treated with LPS containing stimulation media, composed of DMEMc + 500 ng/ml LPS (3), or the PBS control media, composed of DMEMc + an equivalent volume of 1x PBS. Inverted phase contrast micrographs (Zeiss Primovert) with the 40X objective fitted with an Axiocam ERc5s (Zeiss). were used to image the cells at 3-, 24-, and 48-hours post-treatment.

**Stimulation for NLRP3 inflammasome.** To activate the inflammasome, cells were primed with LPS (500 ng/mL) then activated with nigericin (10µM and 15µM, diluted in DMEMc). Three 6-well plates were seeded with 4 x $10^5$ cells per well then incubated for 24 hours. 15 of the 18 wells were treated with LPS stimulation media and the remaining 3 wells were treated with PBS control media. The media from the LPS treated wells was removed after four hours and replaced with the corresponding conditions: PBS stimulation media was added to 3 of the wells, 10µM nigericin stimulation media was added to 6 of the wells, and 15µM nigericin stimulation media was added to the remaining 6 wells. After 2 hours of nigericin treatment, the supernatants were transferred to Eppendorf tubes, and the cells were lysed over ice with 50µL/well of lysis buffer (20mM Tris (pH 8.8), 127mM NaCl, 10% glycerol, 1% Triton X-100, 2mM EDTA, and distilled $H_2O$). The lysates were centrifuged for 10 minutes at 14,000 RPM at 4°C, and the supernatants were centrifuged at 1000 RPM for 3 minutes to remove cell debris before transferring to new tubes. The lysates and supernatants were frozen at -20°C until further use.

**Rg3 treatment of cells.** Four 6-well plates were seeded with 4 x $10^5$ J774A.1 cells/well and grown for 24 hours prior to treatment. The concentrations used for this experiment were 15 µM nigericin, 500 ng/mL LPS, and 5µg/mL ginsenoside Rg3. The media containing the previous treatment was replaced with 2mL of media containing the next treatment. The wells were treated in duplicates as per the conditions in Table 1.

**TABLE. 1** Treatment conditions over an 8-hour period.

| Hour (8hr Timeframe) | 1 | 2 | 3 | 4 | 5 | 6 | 7 | 8 |
|---|---|---|---|---|---|---|---|---|
| **Condition 1 (PBS Only)** | | | PBS | PBS | PBS | PBS | PBS | PBS |
| **Condition 2 (LPS Only)** | | | LPS | LPS | LPS | LPS | PBS | PBS |
| **Condition 3 (Rg3 Only)** | | | | | | | Rg3 | Rg3 |
| **Condition 4 (Rg3-LPS)** | Rg3 | Rg3 | LPS | LPS | LPS | LPS | PBS | PBS |
| **Condition 5 (LPS-Rg3)** | | | LPS | LPS | LPS | LPS | Rg3 | Rg3 |
| **Condition 6 (LPS-N)** | | | LPS | LPS | LPS | LPS | Nigericin | Nigericin |
| **Condition 7 (Rg3 (1hr)-LPS-N)** | | Rg3 | LPS | LPS | LPS | LPS | Nigericin | Nigericin |
| **Condition 8 (Rg3(2hr)-LPS-N)** | Rg3 | Rg3 | LPS | LPS | LPS | LPS | Nigericin | Nigericin |
| **Condition 9 (LPS-N&Rg3(1hr))** | | | | LPS | LPS | LPS | LPS | Nigericin & Rg3 |
| **Condition 10 (LPS-N&Rg3(2hr))** | | | LPS | LPS | LPS | LPS | Nigericin & Rg3 | Nigericin & Rg3 |

At the end of each treatment condition, we collected the culture media for subsequent ELISA experiments, lysed the cells, and handled the samples in the same manner as the stimulation test, with the exception of combining the duplicates together to maximize protein quantity.

**IL-1β and TNF-α ELISA.** The ELISAs were conducted on cell supernatants using the Invitrogen IL-1 beta Mouse Uncoated ELISA Kit (Thermo Fisher, Cat no. 88-7013-88) and Invitrogen TNF alpha Mouse Uncoated ELISA Kit (Thermo Fisher, Cat no. 88-7324-88) according to the manufacturer's instructions. The ELISA wash buffer was prepared using 1X PBS and 0.05% Tween-20. 1M $H_3PO_4$ was used as an ELISA stop buffer (Thermo Fisher, Cat no. SS04).

**SDS-PAGE.** Cell culture supernatants were concentrated using Amicon Ultra-15 Centrifugal Filter Tubes with 10 kDa molecular weight cutoff. Protein concentration was quantified prior to loading using the Pierce BCA Protein Assay Kit (Thermo Fisher, Cat no. 23225), following the manufacturer's instructions. SDS-PAGE gels were made with a 12% acrylamide resolving layer and 4% acrylamide stacking layer. 20µg/well of protein per well was loaded with 4X sample loading buffer (0.25 M Tris-HCl pH 6.8, 8% SDS, 30% Glycerol, and 0.02% Bromophenol Blue containing 0.3M DTT). We used 1x Tris-Glycine SDS-PAGE Electrophoresis buffer as our running buffer and Triton X-100 lysis buffer as a diluent. The Thermo Scientific Spectra Multicolor Broad Range Protein Ladder (Thermo Fisher, Cat no. 26634) was used. The gels ran in SDS-PAGE running buffer at 200V until the loading dye had run off the bottom of the gel (40-50 minutes). The gels were then transferred to an 8 x 5.5 cm Hybond-P:PVDF (polyvinylidene difluoride membrane) at 30V and 4°C overnight in a Towbin buffer (25 mM Tris-HCl pH 8.3, 192 mM glycine, 20% (v:v) methanol).

**Western blotting.** After blocking the membranes with 5% BSA in TBS-T for 45 minutes at room temperature, one membrane was incubated in 1:1000 dilution of goat anti-mouse Il-1β Ab (R&D Systems, Cat no. AF-401-NA) and the second was incubated in 1:1000 monoclonal mouse anti-mouse β-actin Ab (Sigma-Aldrich, Cat no. A5316) for 1 hour. The first membrane was incubated in a 1:10000 dilution of anti-goat IgG Ab HRP conjugate (R&D Systems, Cat no. HAF109) in TBS-T + 1% BSA (Sigma-Aldrich, Cat no. A7906) for 45 minutes. The second membrane was incubated in a 1:10000 dilution of goat anti-mouse IgG Ab H/L:HRP (BioRad, STAR207P) in TBS-T + 1% BSA for 45 minutes. Finally, membranes were treated with a 1:1 solution of luminol and peroxide (Biorad, Cat no. 1705061) for 4 minutes, and then imaged using a ChemiDoc imaging system. Two gels were run with equal amounts of protein loaded but were probed separately for IL-1β and β-actin respectively.

**Visualization of morphology with phase contrast and fluorescence microscopy.** J774A.1 cells were seeded on glass coverslips in a 12-well plate at a density of 0.1 x $10^6$ cells/well. Cells were grown to a confluency of 85% and treated with the same conditions as the 6-well plate Rg3 procedure, with no replicates. After each treatment was completed, the wells were fixed with Pierce 16% Formaldehyde (Thermo Fisher, Cat no. 28906) diluted to 4% as per the manufacturer's instructions and stored in 1x PBS at 4°C. The cells were permeabilized with a 0.25% Triton x-100 solution in 1x PBS + 1% BSA for 10 minutes at room temperature. The wells were then treated with 1:100 dilution of Alexa Fluor 568- phalloidin (Invitrogen, Cat no. A12380) in 1x PBS + 1% BSA for 20 minutes in dark at room temperature to stain the actin cytoskeleton. After rinsing with 1x PBS, 1 ml of PBS and 2 drops of Nuc Green Dead 488 ReadyProbes (Thermo Fisher, Cat no. R37109) were added to each well and the plate was incubated in darkness at room temperature for 25 minutes. Following another 1x PBS rinse, coverslips were mounted to a microscope slide using Invitrogen ProLong Gold Antifade Mountant (Thermo Fisher, Cat no. P36930) and edges were sealed with clear nail polish. The slides were viewed with a fluorescence microscope using 40x and 100x (oil immersion) objectives, and images were captured with a Zeiss Axiocam 202 monochrome camera. Five representative cells (Supplementary Fig. S4) from the actin labeled images for each cell condition (except LPS-N+Rg3(1hr) due to poor image quality), then measured for the length at the longest axis, area, perimeter, and circularity index (0-1) using image J.

## RESULTS

**LPS induced pro-IL-1β upregulation, but nigericin did not produce detectable mature IL-1β.** To determine the optimal conditions for inflammasome activation in J774A.1 macrophages, we analyzed the production of pro-IL-1β and cleaved Il-1β in response to LPS priming and different concentrations and time of nigericin stimulation via western blot. Two identical membranes were primed for either Il-1β or beta-actin. We found that LPS stimulation induced pro-IL-1β production compared to unstimulated controls (Fig.1), but no cleaved IL-1β could be detected in LPS and nigericin treated cells.

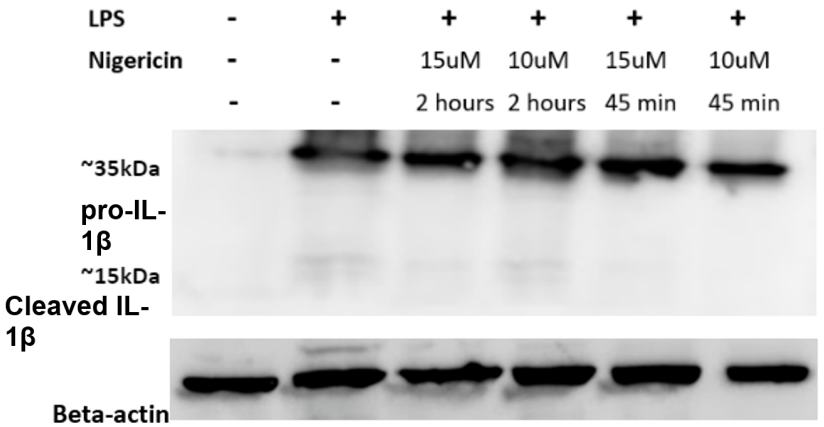


**FIG. 1 Pro-IL-1β is induced in J774A.1 macrophages in response to LPS**. Western Blot Analysis for pro-IL-1β (31kDa) or cleaved IL-1β (17kDa) of cell lysates from J774A.1 macrophages treated with LPS (500 ng/mL) or PBS for 4 hours then stimulated with PBS for 2 hours or nigericin (10uM or 15uM) for 45 min or 2 hours. β-actin is shown as a loading control, probed on a different membrane.

**Exposure to Nigericin leads to increased detection of IL-1β in cell supernatants over both time and concentration.** Because we were unable to detect cleaved IL-1β in our protein lysates, we investigated the cell supernatants to determine if IL-1β was being secreted following nigericin treatment. We used a capture antibody ELISA with three technical replicates to measure the concentration of secreted IL-1β from J774A.1 murine macrophages treated with nigericin for 45 or 120 minutes at 10uM or 15uM concentrations, both after 4 hours of LPS stimulation (Fig. 2). We detected no IL-1β in the supernatants of our PBS and LPS only conditions. We also did not detect any IL-1β in the 10 uM/45 minute nigericin treatment condition. We did observe IL-1β secretion for the other three conditions with concentration increasing with both time and nigericin concentration, to a maximum of 868 pg/mL in our 15uM/120 minute treatment condition. Unfortunately, the ELISA does not differentiate between pro-IL-1β or cleaved IL-1β. Thus, these results possibly indicate that

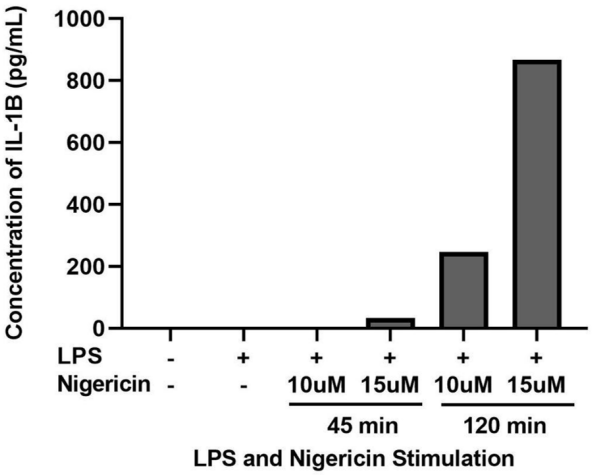


**FIG. 2 Exposure to Nigericin leads to increased secretion of IL-1B over both time and concentration.** J774A.1 macrophage cells were either treated with nigericin for 45 or 120 minutes at 10uM or 15uM concentrations, both after 4 hours of LPS stimulation. Cells were treated with PBS for 4 hours as a negative control. A capture antibody ELISA was used to measure the concentration of secreted IL-1β in cell culture supernatants. The concentration of IL-1β was observed to increase in the nigericin treatment groups compared to the control with the highest amounts secreted at the 15 uM and 120 minute time point.

we did, in fact, create an activated model of the NLRP3 inflammasome, and we are detecting cleaved IL-1β, or it might mean that our cells are dying following nigericin treatment, releasing pro-IL-1β.

**Rg3 affects TNF-α secretion in LPS stimulated cells.** At this point we had been unable to detect cleaved IL-1β following cell stimulation, hence, we decided to focus on the initial priming step of NLRP3 inflammasome activation. TNF-α is a secreted cytokine which is controlled via the NF-κB pathway. Pro-IL-1β, commonly used as a readout for NLRP3 inflammasome priming, is also regulated via the NF-κB pathway, however, is typically not secreted (2). Thus, because they are both regulated via the same pathway, we used TNF-α as a proxy for NLRP3 inflammasome priming. We wanted to test the effects of Rg3 on LPS-dependent TNF-α production and determine if the timing of Rg3 exposure played a role. Therefore, we either pre-treated cells with Rg3 for 2 hours prior to LPS stimulation, or treated cells with Rg3 for 2 hours after LPS stimulation. As expected, untreated cells had low detectable levels of TNF-α in the cultured media, and stimulation with LPS resulted in high levels of detectable TNF-α (Fig. 3). However, treatment with Rg3 either before or after LPS stimulation inhibited the release of TNF-α. This suggests that Rg3 may inhibit a post-transcriptional step of TNF-α release, but further tests would need to be done to test this hypothesis.

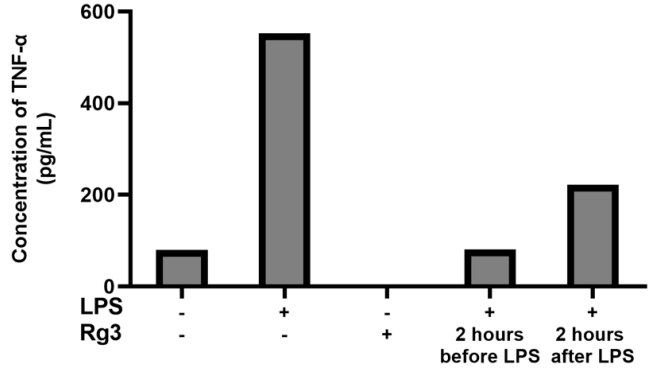


**FIG. 3 Rg3 affects TNF-α secretion in LPS treated cells.** J774A.1 cells were either treated with Rg3 (50uM) for 2 hours followed by 4 hours of LPS priming (500 ng/mL), or cells were primed with LPS for 4 hours followed by treatment with Rg3 for 2 hours. Cells were treated with PBS for 4 hours as a negative control. Cell culture supernatants were collected and a TNF-α ELISA was performed to detect secreted TNF-α.

We also treated cells with Rg3 for 1 or 2 hours followed by 4 hours of LPS priming and 2 hours of nigericin activation. Another set of cells were primed with LPS for 4 hours followed by concurrent treatment with nigericin and Rg3 for 1 or 2 hours. Higher levels of TNF-α are present when cells were treated with Rg3 concurrently with nigericin following LPS treatment compared to when cells were treated with Rg3 before treatment with LPS followed by nigericin (Supplementary Fig. S2). However, our activated control (cells treated with LPS for 4 hours followed by 2 hours with nigericin) had lower than expected levels of TNF-α. If priming occurred as expected in this control, we would expect to see levels of TNF-

α comparable to the LPS-only treated cells. Because of this, we can't be sure of the effect Rg3 is having on TNF-α when we treat cells with both LPS and nigericin.

**Treatment of J774A.1 murine macrophage cells with Rg3 may reduce the morphological effects of LPS and nigericin treatments.** We wanted to determine if there were any noticeable morphological differences between the activated cells with or without Rg3 treatment. We stained the actin cytoskeleton of the cells in each treatment condition, then used fluorescence microscopy to compare their measurements and morphology (Fig. 4). We noticed the cells treated with Rg3 only appear to be healthy and similar to the PBS control in the fluorescence photos. The LPS-Nigericin treated cells seemed to be the most misshapen and had the lowest circularity index based on the ImageJ analysis (Fig. 4D). The LPS only condition had a higher circularity index and was not as misshapen compared to the LPS-Nigericin condition, suggesting that inflammasome activation by nigericin may cause additional morphological changes. The conditions treated with Rg3 first, then LPS and Nigericin appeared to be less misshapen than the LPS-Nigericin condition. This leads us to believe that Rg3 treatment could suppress some of the damaging inflammatory effects of inflammasome activation.

## DISCUSSION

In this study, we set out to develop a model for the activation of the NLRP3 inflammasome in J774A.1 murine macrophage cells, and to identify how ginsenoside Rg3 specifically affects the priming and activation of the NLRP3 inflammasome. While we were unable to detect cleaved Il-1β, indicative of a fully activated NLRP3 inflammasome, we were able to detect pro-IL-1β, indicating successful priming with LPS in J774A.1 cells. Further, we were able to demonstrate the downregulation of TNF-α production in LPS-stimulated cells by ginsenoside Rg3.

**Towards optimizing a model for the activated NLRP3 inflammasome.** Our first goal in this study was to optimize a working model for activation of the NLRP3 inflammasome in J774A.1 murine macrophage cells. Activating the NLRP3 inflammasome is a two-step process, wherein specific PAMPs stimulate NLRs, TLRs or cytokine receptors on resting macrophages, providing the first signal leading to activation of the transcription factor NF-kB which upregulates NLRP3 and pro-IL-1β (2). We used LPS as a PAMP to stimulate cells and found that it did induce pro-IL-1β upregulation compared to the PBS control in cell lysates (Fig. 1). The second signal for NLRP3 inflammasome activation is initiated by PAMPs or DAMPs which leads to the formation of inflammasome resulting in cleavage of pro-IL-1β to mature IL-1β (2). We used nigericin as a DAMP to activate cells and again detected pro-IL-1β in cell lysates (Fig. 1), however, no mature IL-1β was detected. Thus, to test if cleaved IL-1β was being secreted, we performed an ELISA on the cell supernatants and found that exposure to nigericin led to increased secretion of IL-1β over both time and concentration (Fig. 2). Unfortunately, the ELISA doesn't tell us if what we are seeing is pro-IL-1beta or cleaved IL-1beta, resulting in two separate interpretations for what this data might mean. It is possible that we successfully activated signal 2 of the NLRP3 inflammasome and we are indeed detecting secreted IL-1β. However, it could instead be possible that signal 1 is occurring successfully in these cells, resulting in the production of pro-IL-1β, but that these cells are dying following treatment with nigericin and releasing their cytosolic contents, leading to pro-IL-1β being detected in the supernatants. Previous research, however, shows that nigericin is not toxic to the cells at the chosen concentration (15uM) and time (~120 min) (40–42) and only causes cell death when added after LPS pre-treatment. Thus, even if nigericin caused cell death, and release of pro-IL-1β into the supernatant, this mechanism was probably triggered by the inflammasome activation, which causes downstream cell death. In this case, cleaved IL-1β would be present as well as pro-IL-1β, supporting our hypothesis that nigericin causes the activation of the inflammasome and cleavage of pro-IL-1β.

To determine if we were indeed detecting cleaved IL-1β or just pro-IL-1β in our cell culture supernatants, we attempted a western blot on concentrated cell culture supernatant samples (Supplementary Fig. S1). We treated cells with 500 ng/mL of LPS for 4 hours,

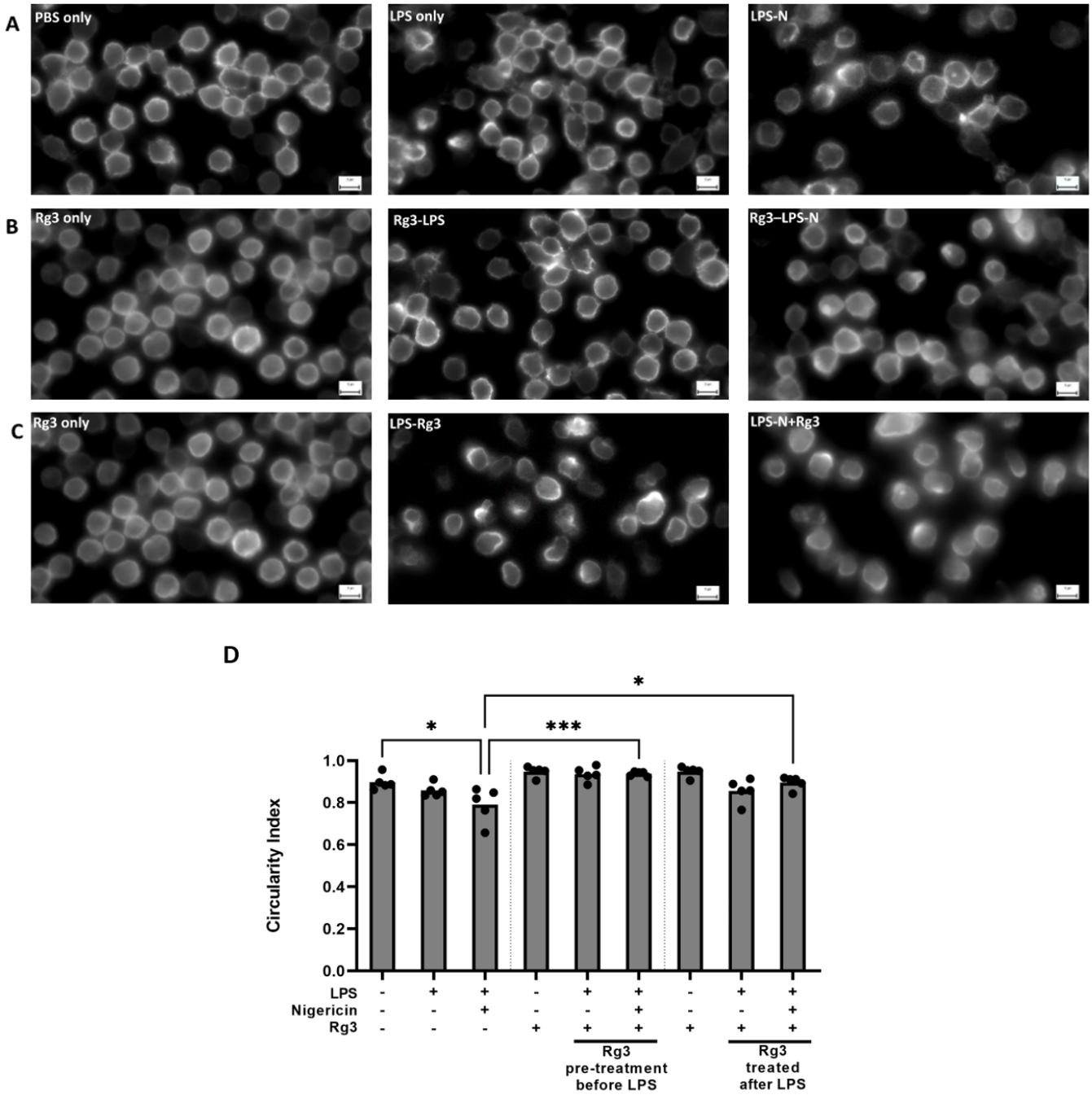


**FIG. 4 Treatment of J774A.1 murine macrophage cells with Rg3 may reduce the morphological effects of LPS and nigericin treatments. (A-C)** J774A.1 cells grown on glass coverslips in DMEMc for 48 hours were treated with the above conditions (x-axis), 4 hours for LPS (500 ng/ml), 2 hours for nigericin (N, 50μM), and 2 hours for ginsenoside Rg3 (5μg/ml), then fixed with 4% formaldehyde, permeabilized with 0.25% Triton x-100, and dyed with Alexa Fluor 568 and Nuc Green Dead 488 before undergoing fluorescence microscopy. These images are of the actin cytoskeleton only (red channel). Cells treated with PBS only (**A**) and ginsenoside Rg3 only (**B,C**) were generally rounded and regular. Cells treated with LPS only and, worst so, LPS then nigericin (**A**) were irregularly shaped and highly variable. Cells treated with Rg3 first, then LPS and PBS or nigericin (**B**) appeared to be more regular and rounded than LPS treated cells without Rg3 treatment. Cells treated with LPS first, then Rg3 with or without nigericin (**C**) seem to be more irregular and variable than the controls (PBS only and Rg3 only) and the cells treated with Rg3 first (**B**). Circularity index of measurements from five representative cells from each condition analyzed by ImageJ (**D**). One-way ANOVA test, P = 0.0040. Tukey's multiple comparison test: only significant data shown on graph, all other pairs ns.

followed by 2 hour treatment with 15uM nigericin, as this was the condition where we detected the highest concentration of IL1b by ELISA. We included a whole cell lysate sample extracted from cells stimulated with LPS as a positive control for pro-IL-1β. We were unable to detect pro or cleaved IL-1β in our cell culture supernatants, contrary to our ELISA results. Further, the presence of a band at 35 kDa in our cell lysates sample indicates the presence of pro-IL-1β, and confirms that our SDS-PAGE and western blot were performed successfully (Supplementary Fig. S1). It is important to note that this experiment was done using culture media containing 10% FBS. Thus, in the process of concentrating the cell culture supernatants much of the protein present may be from components of FBS, and could make it difficult to detect our protein of interest by western blotting. To address this concern, we conducted a follow-up experiment where we eliminated FBS in the media of each of our final conditions. Unfortunately, the ordered Amicon Ultra-15 Centrifugal Filter Tubes did not arrive on time and we were unable to test this hypothesis. However, we hope the problems we faced help outline next steps for future student researchers. Specifically, we believe there is value in optimizing the procedure for detecting cleaved IL-1β in the cell supernatants via Amicon Ultra-15 Centrifugal Filter Tubes and Western blotting.

**Rg3 may have an anti-inflammatory effect on LPS-treated J774A.1 cells.** Our second aim investigated how Rg3 specifically inhibits the NLRP3 inflammasome. Based on previous research, we believed that Rg3 would inhibit the inflammasome both by interfering with signal 1 (priming), by blocking the NF-κB pathway, and signal 2 (activation), by blocking inflammasome assembly (33, 36). Thus, we hypothesized that if Rg3 was added before LPS priming, we would see decreased levels of pro-IL-1β and cleaved IL-1β. However, if Rg3 was added after LPS priming, we hypothesized that we would only see decreased levels of cleaved IL-1β. Because we were unable to develop a fully activated model, we decided to move ahead and determine how Rg3 was affecting priming in our model. Because we had been unable to detect pro-IL-1β in our cell culture supernatants via western blot, and because our IL-1β ELISA could not differentiate between pro-IL-1β and IL-1β, we attempted to use TNF-α as a proxy for NLRP3 inflammasome priming. Priming of the inflammasome (and production of pro-IL-1β) is mediated by the NF-κB pathway (2). The NF-κB pathway also mediates production of TNF-α, however, TNF-α is secreted (43), meaning we could use a TNF-α ELISA on our cell culture supernatants.

We demonstrated that treating J774A.1 cells with Rg3 both before and after LPS leads to decreased TNF-α production compared to LPS-only treated cells (Figure 3). This demonstrates that Rg3 is generally anti-inflammatory. Indeed, the morphology of cells treated with Rg3 prior to or following LPS and nigericin treatment was more regular and has a higher circularity index than cells treated with LPS and nigericin (Fig. 5), further suggesting that Rg3 may prevent some inflammatory effects. However, further studies are needed to link this anti-inflammatory effect to the NF-κB pathway and the NLRP3 inflammasome.

We also attempted to determine how Rg3 affects TNF-α secretion in cells treated with nigericin. Treating cells with Rg3 before LPS and nigericin led to lower levels of TNF-α compared to when cells were treated with Rg3 concurrently with nigericin following LPS treatment (Supplementary Fig. S2). However, it is important to note that our positive control for these conditions (cells treated with LPS for 4 hours followed by 2 hours with nigericin) had much lower levels of TNF-α than previous researchers have found (44), making interpretation of these results difficult. If our model was being effectively primed, we would expect to see comparable levels of TNF-α in our LPS-only condition and our LPS followed by nigericin treatment. One reason we may have had such low levels of TNF-α in our positive control is due to low cell confluency. The cell confluency, both before and after treatment, was much lower for the cells treated with LPS followed by nigericin compared to the LPS-only condition (where cells were treated with PBS following LPS) (Supplementary Fig. S3).

**Limitations** The main limitation in our study was our inability to establish signal 2 activation of NLRP3 in our Western blot procedures. Our Western blot on whole cell lysates did not detect a band for cleaved IL-1β which may be due to the sensitivity limitations western blotting technique to detect potentially low quantities of the cleaved product in the cell lysates. Previous research has successfully observed bands for cleaved IL-1β wherein they

loaded 50 ug of protein per well (45). Similarly, a study which used ATP as an activator also detected visibly large bands of cleaved IL-1β in their western blot (46). However, in our study, we were able to load only 20 ug of protein per well which could have been too low for adequate detection.

Because the literature strongly supports nigericin as a potent activator of the NLRP3 inflammasome, this suggests the improper functioning of our model (4). While our ELISA results on IL-1β may indicate the secretion of cleaved IL-1β, we were unable to support this with a Western blot on cell supernatants (Supplementary Fig. S1). Further, the cells following LPS and nigericin treatment (Supplementary Fig. S3) did not have characteristic membrane bubbling indicative of pyroptosis that other researchers have observed (38, 47). Additionally, prior research on NLRP3 inflammasome activation makes use of primary bone marrow derived macrophages (BMDMs) (48), B cells (49) or microglia (50) wherein they successfully measure cleaved cytokine readouts. Future studies could explore using these other cell lines while also optimizing J774A.1 cell response as they have been successfully used in prior research (38). This highlights the need to explore how the use of over-passaged cell lines could contribute to irregularity in inflammasome activation (51).

Further, our exclusive readout of IL-1β as indicative of signal 2 activation limits our findings. NLRP3 inflammasome activation is a complex process, with multiple possible readouts such as blots of cleaved IL-1β or Caspase 1, NLRP3 protein, or ASC speck formation - to confirm inflammasome activation (4, 33, 42, 44). Therefore, searching for multiple indicators of activation would increase the likelihood of detecting signal 2 activation.

Due to the inability to establish a working model, we were unable to test how Rg3 specifically affects the NLRP3 inflammasome. While our results may indicate a general anti-inflammatory role of Rg3 on J774A.1 cells, as indicated by decreed TNF-α secretion and more regular cell morphology, we were unable to test how these readouts pertain to the NLRP3 inflammasome.

**Conclusions** In this study, we were able to detect successful priming of the NLRP3 inflammasome in J774A.1 cells via western blot for pro-IL-1β on cell lysates following treatment with 500 ng/ml of LPS for 4 hours. We were unable to successfully detect cleaved IL-1β in J774A.1 cells treated with 10uM or 15uM of nigericin for 45 minutes or 2 hours following LPS priming. However, our results indicate that troubleshooting the western blot procedure for cell supernatants may be a valuable pursuit in future research projects. Additionally, we were able to demonstrate that Rg3 inhibits TNF-α secretion in LPS-stimulated J774A.1 cells.

**Future Directions** As previously suggested, future research should prioritize the development of a working model of the fully activated NLRP3 inflammasome. Future studies should work towards obtaining higher amounts of protein in their cell lysates to adequately test for cytokine upregulation. One potential solution is to allow cells to grow to a higher confluency before stimulation with LPS. Our results indicate that there may be a benefit in optimizing procedures for the detection of cleaved IL-1β in cell supernatants via Western blot. Specifically, removing FBS in cell media for the treatment preceding supernatant collection may allow for better detection of cell secreted proteins. Further, the use of Amicon Ultra-15 Centrifugal Filter Tubes for the protein concentration of supernatants appears to be a valuable method that may require less time and troubleshooting than other methods, such as the chloroform/methanol precipitation method.

## ACKNOWLEDGEMENTS

We would like to acknowledge Dr. Marcia Graves and Dr. Mihai Cirstea for their unconditional support and guidance throughout the entire process, without whom this project would not have been possible. Additionally, we would like to thank Jade Muileboom for her motivation, support and guidance in the laboratory. We would also like to thank teams 2 Epsilon and 2 Gamma for creating a collaborative environment and being wonderful company during extensive hours in the lab. We would like to acknowledge Dr. David Oliver for providing advice and being a constant support. Lastly, we would like to acknowledge the

UBC Department of Microbiology & Immunology for their support in funding our experiments.

## REFERENCES


1. **Hughes MM, O'Neill LAJ**. 2018. Metabolic regulation of NLRP3. *Immunol Rev* **281**:88–98.
2. **Swanson KV, Deng M, Ting JP-Y**. 2019. The NLRP3 inflammasome: molecular activation and regulation to therapeutics. *Nat Rev Immunol* **19**:477–489.
3. **Eisenbarth SC, Colegio OR, O'Connor W, Sutterwala FS, Flavell RA**. 2008. Crucial role for the Nalp3 inflammasome in the immunostimulatory properties of aluminium adjuvants. *Nature* **453**:1122–1126.
4. **Mariathasan S, Weiss DS, Newton K, McBride J, O'Rourke K, Roose-Girma M, Lee WP, Weinrauch Y, Monack DM, Dixit VM**. 2006. Cryopyrin activates the inflammasome in response to toxins and ATP. *Nature* **440**:228–232.
5. **Armstrong H, Bording-Jorgensen M, Chan R, Wine E**. 2019. Nigericin Promotes NLRP3-Independent Bacterial Killing in Macrophages. *Frontiers Immunol* **10**. doi: 10.3389/fimmu.2019.02296.
6. **Ren K, Torres R**. 2009. Role of interleukin-1β during pain and inflammation. *Brain Res Rev* **60**:57–64.
7. **Rosales C**. 2018. Neutrophil: a cell with many roles in inflammation or several cell types? *Front Physiol* **9**. doi: 10.3389/fphys.2018.00113.
8. **Den Hartigh AB, Fink SL**. 2018. Detection of inflammasome activation and pyroptotic cell death in murine bone marrow-derived macrophages. *J Vis Exp* **135**:e57463.
9. **Tahoun A, Jensen K, El-Sharkawy H, Gally D, Rizk AM, Ajarem J, Allam A, Mahmoud AM**. 2020. Inflammasome activation in bovine peripheral blood-derived macrophages is associated with actin rearrangement. *Animals (Basel)* **10**:e655.
10. **Coll RC, O'Neill L, Schroder K**. 2016. Questions and controversies in innate immune research: what is the physiological role of NLRP3? *Cell Death Discov* **2**:e16019.
11. **Chen KW, Schroder K**. 2013. Antimicrobial functions of inflammasomes. *Curr Opin Microbiol* **16**:311–318.
12. **Clay GM, Sutterwala FS, Wilson ME**. 2014. NLR proteins and parasitic disease. *Immunol Res* **59**:142–152.
13. **Rajamäki K, Lappalainen J, Oörni K, Välimäki E, Matikainen S, Kovanen PT, Eklund KK**. 2010. Cholesterol crystals activate the NLRP3 inflammasome in human macrophages: a novel link between cholesterol metabolism and inflammation. *PLoS One* **5**:e11765.
14. **Westermark P, Andersson A, Westermark GT**. 2011. Islet amyloid polypeptide, islet amyloid, and diabetes mellitus. *Physiol Rev* **91**:795–826.
15. **Martinon F, Pétrilli V, Mayor A, Tardivel A, Tschopp J**. 2006. Gout-associated uric acid crystals activate the NALP3 inflammasome. *Nature* **440**:237–241.
16. **Ito S, Hara Y, Kubota T**. 2014. CARD8 is a negative regulator for NLRP3 inflammasome, but mutant NLRP3 in cryopyrin-associated periodic syndromes escapes the restriction. *Arthritis Res Ther* **16**:R52. doi: 10.1186/ar4483
17. **Stienstra R, Tack CJ, Kanneganti T-D, Joosten LAB, Netea MG**. 2012. The inflammasome puts obesity in the danger zone. *Cell Metab* **15**:10–18.
18. **Koenen TB, Stienstra R, van Tits LJ, Joosten LAB, van Velzen JF, Hijmans A, Pol JA, Van der Vliet JA, Netea MG, Tack CJ, Stalenhoef AFH, de Graaf J**. 2011. The inflammasome and caspase-1 activation: a new mechanism underlying increased inflammatory activity in human visceral adipose tissue. *Endocrinology* **152**:3769–3778.
19. **Stienstra R, Joosten LAB, Koenen T, van Tits B, van Diepen JA, van den Berg SAA, Rensen PCN, Voshol PJ, Fantuzzi G, Hijmans A, Kersten S, Müller M, van den Berg WB, van Rooijen N, Wabitsch M, Kullberg B-J, van der Meer JWM, Kanneganti T, Tack CJ, Netea MG**. 2010. The inflammasome-mediated caspase-1 activation controls adipocyte differentiation and insulin sensitivity. *Cell Metab* **12**:593–605.
20. **Giordano A, Murano I, Mondini E, Perugini J, Smorlesi A, Severi I, Barazzoni R, Scherer PE, Cinti S**. 2013. Obese adipocytes show ultrastructural features of stressed cells and die of pyroptosis. *J Lipid Res* **54**:2423–2436.
21. **Finch CE**. 2010. Evolution in health and medicine Sackler colloquium: evolution of the human lifespan and diseases of aging: roles of infection, inflammation, and nutrition. *Proc Natl Acad Sci USA* **107** Suppl 1:1718–1724.
22. **Robbins GR, Wen H, Ting JP-Y**. 2014. Inflammasomes and metabolic disorders: old genes in modern diseases. *Mol Cell* **54**:297–308.
23. **CDC**. 2022. National Diabetes Statistics Report. www.cdc.gov/diabetes/data/statistics-report/index.html. Retrieved 18 December 2022.
24. **Government of Canada SC**. 2022. Leading causes of death, total population, by age group. www150.statcan.gc.ca/t1/tbl1/en/tv.action?pid=1310039401. Retrieved 6 January 2023.
25. **CDC**. 2022. Heart Disease | cdc.gov. Centers for Disease Control and Prevention. www.cdc.gov/heartdisease/index.htm. Retrieved 6 January 2023.

26. **Government of Canada SC**. 2019. Overweight and obese adults, 2018. www150.statcan.gc.ca/n1/pub/82-625-x/2019001/article/00005-eng.htm. Retrieved 6 January 2023.
27. **Diabetes Canada**. 2022. Diabetes rates continue to climb in Canada. www.diabetes.ca/media-room/press-releases/diabetes-rates-continue-to-climb-in-canada. Retrieved 6 January 2023.
28. **Jia L, Zhao Y, Liang X-J**. 2009. Current evaluation of the millennium phytomedicine- ginseng (II): Collected chemical entities, modern pharmacology, and clinical applications emanated from traditional Chinese medicine. *Curr Med Chem* **16**:2924–2942.
29. **Tang Y-C, Zhang Y, Zhou J, Zhi Q, Wu M-Y, Gong F-R, Shen M, Liu L, Tao M, Shen B, Gu D-M, Yu J, Xu M-D, Gao Y, Li W**. 2017. Ginsenoside Rg3 targets cancer stem cells and tumor angiogenesis to inhibit colorectal cancer progression in vivo. *Int J Oncol* **52**:127–138.
30. **Sun M, Ye Y, Xiao L, Duan X, Zhang Y, Zhang H**. 2017. Anticancer effects of ginsenoside Rg3 (Review). International Journal of Molecular Medicine **39**:507–518.
31. **Wang J, Tian L, Khan MN, Zhang L, Chen Q, Zhao Y, Yan Q, Fu L, Liu J**. 2018. Ginsenoside Rg3 sensitizes hypoxic lung cancer cells to cisplatin via blocking of NF-κB mediated epithelial-mesenchymal transition and stemness. *Cancer Lett* **415**:73–85.
32. **Zheng X, Chen W, Hou H, Li J, Li H, Sun X, Zhao L, Li X**. 2017. Ginsenoside 20(S)-Rg3 induced autophagy to inhibit migration and invasion of ovarian cancer. *Biomed pharmacother* **85**:620–626.
33. **Shi Y, Wang H, Zheng M, Xu W, Yang Y, Shi F**. 2020. Ginsenoside Rg3 suppresses the NLRP3 inflammasome activation through inhibition of its assembly. *FASEB J* **34**:208–221.
34. **Ren B, Feng J, Yang N, Guo Y, Chen C, Qin Q**. 2021. Ginsenoside Rg3 attenuates angiotensin II-induced myocardial hypertrophy through repressing NLRP3 inflammasome and oxidative stress via modulating SIRT1/NF-κB pathway. *Int Immunopharmacol* **98**:107841.
35. **Luo M, Yan D, Sun Q, Tao J, Xu L, Sun H, Zhao H**. 2020. Ginsenoside Rg1 attenuates cardiomyocyte apoptosis and inflammation via the TLR4/NF-kB/NLRP3 pathway. *J Cell Biochem* **121**:2994–3004.
36. **Kim J, Ahn H, Han B-C, Lee S-H, Cho Y-W, Kim CH, Hong E-J, An B-S, Jeung E-B, Lee G-S**. 2014. Korean red ginseng extracts inhibit NLRP3 and AIM2 inflammasome activation. *Immunol Lett* **158**:143–150.
37. **Dana HM, Rosen A, Tabassi P**. 2022. Towards optimizing ATP-induced activation of the NLRP3 inflammasome in glycolysis-inhibited J774A.1 murine macrophages. *UJEMI* **27**.
38. **Cortez SN, He JY, Lising VM**. 2022. Establishing a J774A.1 murine macrophage NLRP3 inflammasome model for examining short-chain fatty acid suppression. *UJEMI* **27**.
39. **Sekhon P, Singh R, Song A**. 2022. Investigating the role of calcium ion mobilization in NLRP3 inflammasome activation of J774A.1 macrophages and optimizing cell morphology and IL-1β quantification protocols. *UJEMI* **27**.
40. **Su C-C, Wang S-C, Chen I-C, Chiu F-Y, Liu P-L, Huang C-H, Huang K-H, Fang S-H, Cheng W-C, Huang S-P, Yeh H-C, Liu C-C, Lee P-Y, Huang M-Y, Li C-Y**. 2021. Zerumbone suppresses the LPS-induced inflammatory response and represses activation of the NLRP3 inflammasome in macrophages. *Front Pharmacol* **12**. doi: 10.3389/fphar.2021.652860.
41. **Lin Y, Luo T, Weng A, Huang X, Yao Y, Fu Z, Li Y, Liu A, Li X, Chen D, Pan H**. 2020. Gallic acid alleviates gouty arthritis by inhibiting NLRP3 inflammasome activation and pyroptosis through enhancing Nrf2 signaling. *Front Immunol* **11**:e580593.
42. **Hung Y-L, Wang S-C, Suzuki K, Fang S-H, Chen C-S, Cheng W-C, Su C-C, Yeh H-C, Tu H-P, Liu P-L, Huang M-Y, Li C-Y**. 2019. Bavachin attenuates LPS-induced inflammatory response and inhibits the activation of NLRP3 inflammasome in macrophages. *Phytomedicine* **59**:e152785.
43. **Sun X, He X, Tzipori S, Gerhard R, Feng H**. 2009. Essential role of the glucosyltransferase activity in *Clostridium difficile* toxin-induced secretion of TNF-α by macrophages. *Microb Pathog* **46**:298–305.
44. **Song D, Zhao J, Deng W, Liao Y, Hong X, Hou J**. 2018. Tannic acid inhibits NLRP3 inflammasome-mediated IL-1β production via blocking NF-κB signaling in macrophages. *Biochem Biophys Res Commum* **503**:3078–3085.
45. **Hsieh C-Y, Li L-H, Lam Y, Fang Z, Gan CH, Rao YK, Chiu H-W, Wong W-T, Ju T-C, Chen F-H, Chernikov OV, Liu M-L, Hsu C-H, Hua K-F**. 2020. Synthetic 4-hydroxy auxarconjugatin B, a novel autophagy inducer, attenuates gouty inflammation by inhibiting the NLRP3 inflammasome. *Cells* **9**:e279.
46. **Liu X, Zhang X, Ding Y, Zhou W, Tao L, Lu P, Wang Y, Hu R**. 2017. Nuclear factor E2-related factor-2 negatively regulates NLRP3 inflammasome activity by inhibiting reactive oxygen species-induced NLRP3 priming. *Antioxid Redox Signal* **26**:28–43.
47. **Zhang Y, Chen X, Gueydan C, Han J**. 2018. Plasma membrane changes during programmed cell deaths. *Cell Res* **28**:9–21.
48. **Qin N, Xu G, Wang Y, Zhan X, Gao Y, Wang Z, Fu S, Shi W, Hou X, Wang C, Li R, Liu Y, Wang J, Zhao H, Xiao X, Bai Z**. 2021. Bavachin enhances NLRP3 inflammasome activation induced by ATP or nigericin and causes idiosyncratic hepatotoxicity. *Front Med* **15**:594–607.
49. **Alphonse MP, Duong TT, Shumitzu C, Hoang TL, McCrindle BW, Franco A, Schurmans S, Philpott DJ, Hibberd ML, Burns J, Kuijpers TW, Yeung RSM**. 2016. Inositol-

triphosphate 3-kinase C mediates inflammasome activation and treatment response in Kawasaki disease. *J Immunol* **197**:3481–3489.

50. **Lai M, Yao H, Shah SZA, Wu W, Wang D, Zhao Y, Wang L, Zhou X, Zhao D, Yang L**. 2018. The NLRP3-caspase 1 inflammasome negatively regulates autophagy via TLR4-TRIF in prion peptide-infected microglia. *Front Aging Neurosci* **10**:116.

51. **Hughes P, Marshall D, Reid Y, Parkes H, Gelber C**. 2007. The costs of using unauthenticated, over-passaged cell lines: how much more data do we need? *BioTechniques* **43**:575, 577–578, 581-582 passim. doi: 10.2144/000112598.